Shape resonance behavior in $1\pi_g$ photoionization of O_2

M Braunstein and V. McKoy
A. A. Noyes Laboratory of Chemical Physics, California Institute of Technology, Pasadena, California 91125

(Received 10 October 1988; accepted 9 November 1988)

We report calculations of vibrationally resolved cross sections and photoelectron angular distributions for photoionization of O_2 leading to the $X\,^2\Pi_g$ ($v^+ = 0$–4) states of O_2^+ using Hartree–Fock continuum photoelectron orbitals. These studies were motivated by recent results which show that a σ_u shape resonance plays a dominant role in producing non-Franck–Condon vibrational distributions in resonant multiphoton ionization of O_2 via the $C\,^3\Pi_g$ ($1\pi_g 3s\sigma_g$) Rydberg state. In the present study, we investigate how this shape resonance influences photoionization dynamics in single-photon ionization. Below 21 eV photon energy, we find significant non-Franck–Condon effects in the vibrational branching ratios as well as in the vibrationally resolved photoelectron angular distributions. Substantial autoionization hinders a direct comparison between theory and experiment.

I. INTRODUCTION

Recent resonant multiphoton ionization studies via the $C\,^3\Pi_g$ ($1\pi_g 3s\sigma_g$) state of O_2 have shown that a shape resonance has a substantial influence on the vibrational distribution of the ground state $X\,^2\Pi_g$ ion.[1-4] For single-photon ionization leading to the same ion, however, experimental evidence of any corresponding shape-resonant feature is inconclusive. Experimental studies of O_2 in the near-threshold region by single-photon ionization is complicated by extensive autoionization features[5,6] which, to date, have hindered assessment of the possible role of a low-energy shape resonance in the photoionization dynamics. To some extent this complication was avoided in the resonant multiphoton ionization studies[1-4] through specific and limited selection of the photon wavelength.

To further elucidate the role of the σ_u shape resonance in single-photon ionization, we have calculated vibrationally resolved cross sections and photoelectron angular distributions for photoionization leading to the $X\,^2\Pi_g$ state of O_2^+ using frozen-core Hartree–Fock photoelectron orbitals.[7,8] These results show that a σ_u shape resonance becomes very evident in the cross section near the ionization threshold as the internuclear distance R is decreased. This dependence of the transition moment on R, particularly for R values less than R_e of O_2 in this case, leads to significant deviations in the calculated branching ratios from Franck–Condon values for energies from theshold to $\sim$21 eV. The non-Franck–Condon effects are also apparent in our photoelectron asymmetry parameters. Comparison and subsequent interpretation of existing measured branching ratios (obtained from line-source measurements) is inconclusive, giving impetus for measurements that employ tunable radiation and extend to the ionization threshold.

An outline of the paper is as follows. In Sec. II we briefly discuss the Schwinger variational method used to obtain the Hartree–Fock photoelectron orbitals and the procedures with which we obtain our vibrationally resolved cross sections and photoelectron angular distributions. In Sec. III our results are discussed and compared with available experimental data, and in Sec. IV concluding remarks are given.

II. METHOD AND CALCULATIONS

The continuum wave functions were obtained using the iterative Schwinger variational method[7,8] to solve the one-electron Schrödinger equation which the photoelectron orbitals satisfy in the frozen-core Hartree–Fock approximation. In this procedure, the (l,m) partial-wave component of the continuum orbital is given by the equation[8]

$$\psi_{klm}^{(0)}(\mathbf{r}) = \phi_{klm}^{c}(\mathbf{r}) + \sum_{i,j} \langle \mathbf{r}|G_c^{(-)}U|\alpha_i\rangle \times [D^{-1}]_{ij}\langle\alpha_j|U|\phi_{klm}^{c}\rangle, \quad (1)$$

where

$$D_{ij} = \langle\alpha_i|U - UG_c^{(-)}U|\alpha_j\rangle, \quad (2)$$

U is twice the static-exchange interaction potential of the ion core with the Coulomb potential removed, $G_c^{(-)}$ is the Coulomb Green's function, ϕ_{klm}^{c} is the (l,m) component of the Coulomb scattering function, and the α's are discrete basis functions, the same as those used in Ref. 9. This large basis was sufficient to obtain well-converged results without resorting to an iterative procedure for improving $\psi_{klm}^{(0)}$.[8] All integrations were carried out via partial-wave expansions with the resulting radial integrals evaluated by Simpson's rule. The parameters used in the expansion of the static-exchange potential were the same as those in our previous studies of O_2 (Ref. 9) except that the maximum l included in the expansion of the occupied orbitals in the exchange terms were made slightly larger so that $l_i^{ex} = 24\ (1\sigma_g), 24\ (1\sigma_u), 14\ (2\sigma_g), 14\ (2\sigma_u), 12\ (3\sigma_g), 12\ (1\pi_u), 12\ (1\pi_g)$. The grid used to compute the radial integrals consisted of 900 points and extended out to 96.0 a.u. The continuum solutions are constrained to be orthogonal to the bound orbitals of the same symmetry. More details can be found in earlier studies.[7]

The Hartree–Fock wave function for O_2 was constructed from a $[9s5p]/(4s3p)$ contracted Gaussian basis set[10] and two d-type polarization functions with exponents of 2.7040 and 0.5350.[11] The Hartree–Fock energy with this basis at the equilibrium internuclear distance of 2.282 a.u. is $-149.634\,130$ a.u.

 0021-9606/89/052575-05$02.10

We have obtained the photoionization transition matrix elements in both the dipole-length form

$$I^{L}_{lm\mu}(R) = k^{1/2}\langle\Psi_i(\mathbf{r}, R)|\mathbf{r}_\mu|\Psi^{(-)}_{f,klm}(\mathbf{r}, R)\rangle, \quad (3)$$

and the dipole-velocity form

$$I^{V}_{lm\mu}(R) = (k^{1/2}/E)\langle\Psi_i(\mathbf{r}, R)|\nabla_\mu|\Psi^{(-)}_{f,klm}(\mathbf{r}, R)\rangle \quad (4)$$

at the internuclear distances listed in Table I. In Eqs. (3) and (4), Ψ_i represents the initial N-electron wave function and Ψ_f is the wave function for the final ionized state, i.e., an $N-1$ molecular ion plus photoelectron, R specifies the nuclear coordinates, and r stands collectively for all electronic coordinates. These matrix elements were then interpolated with a cubic spline function. The length and velocity forms of the cross section for ionization of the $v=0$ level of O_2 to the nth vibrational state of O_2^+ are then given by

$$\sigma^{L,V}_{v=0,\,v^+=n} = \frac{4\pi^2}{3c}E\sum_{lm\mu}|\langle\chi_i^{v=0}|I^{L,V}_{lm\mu}|\chi_f^{v^+=n}\rangle|^2, \quad (5)$$

where χ are appropriate vibrational wave functions, E is the photon energy, and c is the speed of light. The vibrationally resolved photoelectron asymmetry parameter $\beta_{\hat{k}}$ is defined from the photoelectron differential cross section by

$$\frac{d\sigma^{L,V}_{v=0,\,v^+=n}}{d\Omega_{\hat{k}}} = \frac{\sigma^{L,V}_{v=0,\,v^+=n}}{4\pi} \times[1+\beta^{L,V}_{k,\,v=0,\,v^+=n}P_2(\cos\theta)], \quad (6)$$

where θ is the angle between the direction of polarization of the light and the photoelectron momentum.

The vibrational wave functions were obtained by numerical integration of the Schrödinger equation using the Rydberg–Klein–Rees potentials of Krupenie.[12] The Franck–Condon factors thus obtained agreed with those of Ref. 12, i.e. $(v=0,v^+=0)=0.1884$, $(v=0,v^+=1)=0.3645$, $(v=0,v^+=2)=0.2901$, $(v=0,v^+=3)=0.1227$, $(v=0,v^+=4)=0.0298$.

III. RESULTS AND DISCUSSION

In previous studies of O_2, a σ_u shape resonance has been assigned experimentally[13,14] and investigated theoretically in near-threshold $3\sigma_g$ photoionization.[9,15–18] For $1\pi_g$ photoionization, an earlier fixed-nuclei Stieltjes moment theory (SMT) study showed an apparently weak set of $n\sigma_u$ transitions converging to the first ionization threshold.[17] From consideration of the energy dependence of the quantum defect associated with these states, the spectral distribution of these transitions actually display the onset of resonance behavior and connect smoothly[19] to the adjoining $k\sigma_u$ continuum, as illustrated in Fig. 1. However, the magnitude and variation of the $k\sigma_u$ partial cross section is masked by large nonresonant $k\pi_u$ and $k\delta_u$ contributions to the total cross section. The larger equilibrium internuclear distance of O_2 ($R_e = 2.282$ a.u.) compared to N_2 ($R_e = 2.068$ a.u.) and CO ($R_e = 2.132$ a.u.), where the σ shape resonance is well above threshold, shifts the resonance down to near thresh-

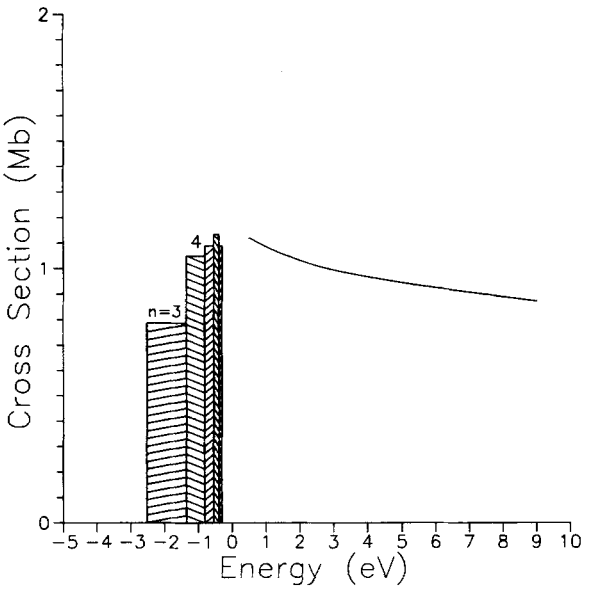

FIG. 1. Oscillator strength distribution in the discrete and continuous spectra for the $1\pi_g \rightarrow \sigma_u$ transition at R_e. The energy scale is relative to the ionization threshold at 12.07 eV. Calculations of Ref. 17 were used to construct the discrete part and the present results (dipole length) are shown above threshold.

TABLE I. Internuclear geometries of O_2 at which photoionization matrix elements were evaluated.

Continuum symmetry	Internuclear distance (a.u.)
$k\sigma_u$[a]	1.8, 1.9, 2.0, 2.1, 2.14, 2.182, 2.232, 2.282, 2.382, 2.482, 2.6
$k\pi_u$	1.8, 2.1, 2.282, 2.6
$k\delta_u$	1.8, 2.1, 2.282, 2.6

[a]Resonant channel.

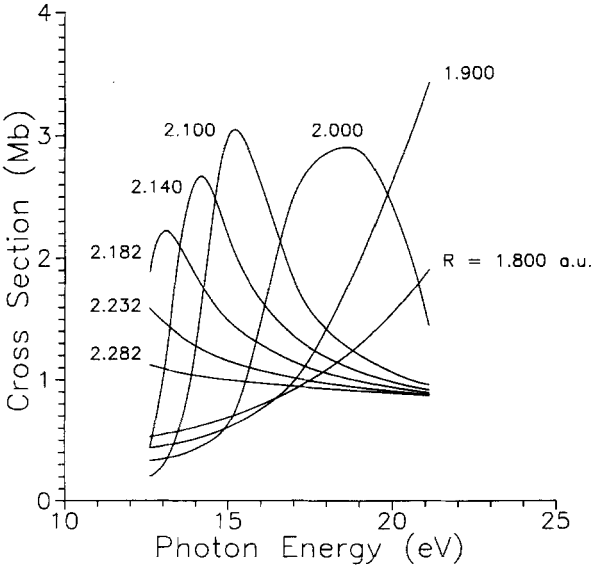

FIG. 2. Photoionization cross sections (dipole length) for the $1\pi_g \rightarrow k\sigma_u$ channel in O_2 at several values of the internuclear distance.

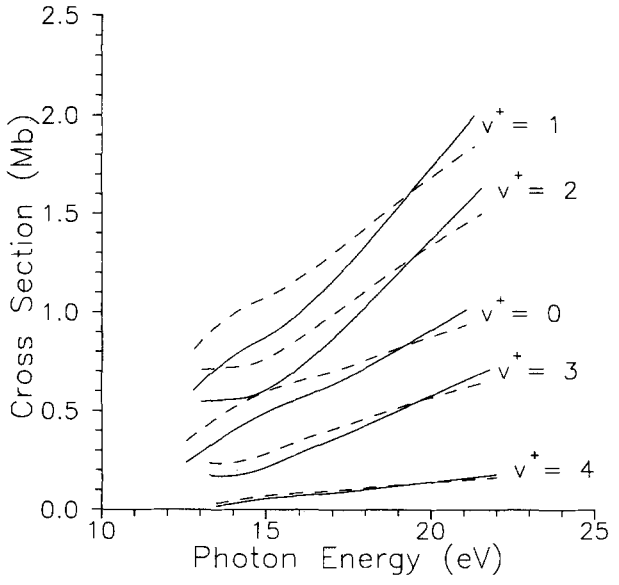

FIG. 3. Vibrationally resolved cross sections leading to the $X\,^2\Pi_g$ state of O_2^+: —, present results (dipole length); ---, present results (dipole velocity).

old, obscuring its presence.

For purposes of illustration, in Fig. 2 we show the $k\sigma_u$ partial cross sections for photoionization out of the $1\pi_g$ orbital of O_2 at eight internuclear distances. The photon energy scale in this figure assumes an ionization potential of 12.07 eV. The dependence of the shape-resonant cross section on internuclear distance is as expected,[20–23] becoming broader and shifting to higher energy as the internuclear distance is decreased. This dependence leads to non-Franck–Condon behavior in the calculated ionic vibrational distributions. In Fig. 3 we show the vibrationally resolved photoionization cross sections for the $v^+ = 0$–4 states of the $X\,^2\Pi_g$ ion. The

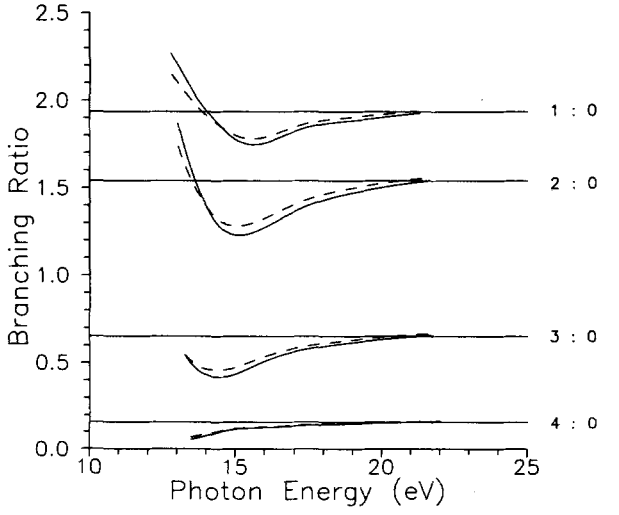

FIG. 4. Vibrational branching ratios for photoionization leading to the $X\,^2\Pi_g$ state of O_2^+: —, present results (dipole length); ---, present results (dipole velocity). The horizontal lines are the Franck–Condon values.

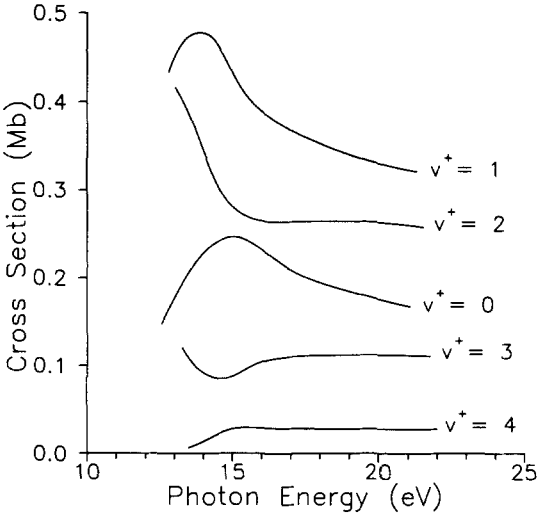

FIG. 5. Vibrationally resolved photoionization cross sections for the $1\pi_g \rightarrow k\sigma_u$ transition (dipole length).

shape resonance partially obscured by the nonresonant $k\pi_u$ and $k\delta_u$ channels, appears as a weak feature in the total cross section at low energy. These variations are sufficient to cause significant deviations from Franck–Condon values in the branching ratios, $\sigma(v=0\rightarrow v^+=n)/\sigma(v=0\rightarrow v^+=0)$, at energies below 21 eV photon energy. We use the notation n:0 to denote the branching ratio for the nth vibrational level. As seen in Fig. 4 the non-Franck–Condon behavior is quite substantial near threshold but by 21 eV the branching ratios reach their Franck–Condon values. For the

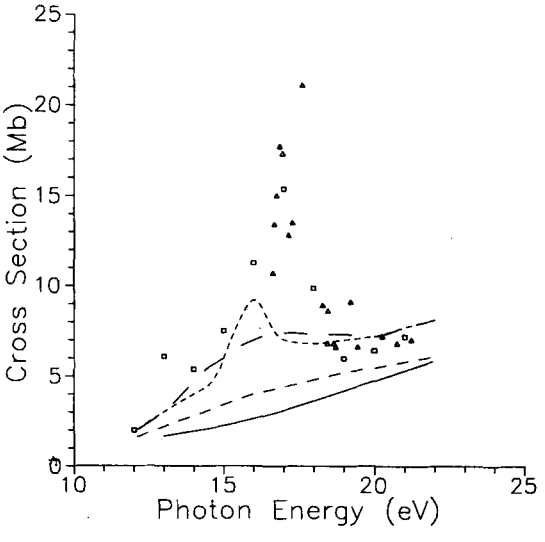

FIG. 6. Photoionization cross section for the $X\,^2\Pi_g$ state of O_2^+: —, present results (dipole length) obtained by summing contributions from $v^+ = 0$–4 vibrational levels; --- (short dash), fixed-nuclei results of Ref. 15 at R_e (MSM); — — — (long dash), vibrationally averaged results of Ref. 15 (MSM); – – – (medium dash), fixed-nuclei results of Ref. 17 at R_e (SMT); □ experimental (e, $2e$) results of Brion *et al.* (Ref. 6); △, experimental line-source results of Samson *et al.* (Ref. 5). Our fixed-nuclei results at R_e are nearly identical to our vibrationally summed results and are not shown.

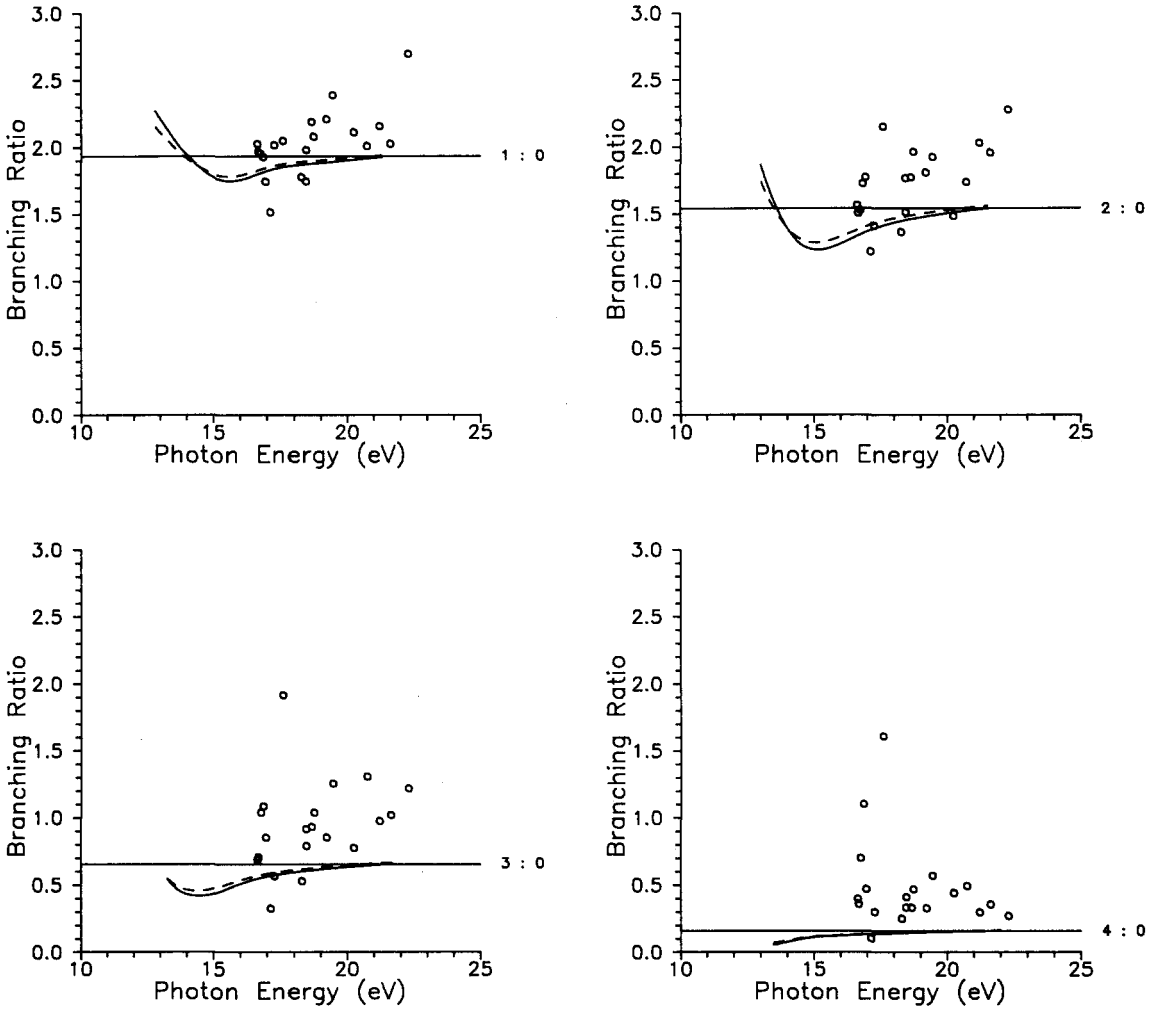

FIG. 7. The same as Fig. 4, plus the experimental line-source data of Gardner *et al.* (Ref. 26) shown by the symbol O.

lower vibrational levels ($v^+ = 0$–2), the behavior of the branching ratios can be understood by examining the dependence of the integrand in Eq. (5) on internuclear distance for the shape-resonant σ_u channel. For these levels the integrand is strongly peaked around one value of the internuclear distance R for the energy range studied. As the vibrational level increases, the largest contribution to the integrand comes from increasing values of R. The resulting shape-resonant σ_u cross sections peak at successively lower values of the photoelectron kinetic energy for increasing vibrational excitation. This behavior is best illustrated in Fig. 5 by showing vibrationally resolved $k\sigma_u$ partial cross sections. The ratios of the total cross sections therefore give rise to the sharp increase at threshold and dip at $\sim$15.0 eV photon energy for the 1:0 and 2:0 branching ratios. For the higher ionic vibrational levels, larger internuclear distances are sampled, but the behavior of the integrands is more complex and cannot be as straightforwardly interpreted.

In Fig. 6 we show the vibrationally summed cross sections for $v^+ = 0$–4. Our results calculated at equilibrium geometry are nearly identical to the vibrationally summed results and are not shown. We also show both the fixed-nuclei results at R_e and the vibrationally averaged cross sections of the multiple scattering model (MSM) study of Dittman *et al.*[15], and the fixed-nuclei results at equilibrium of the SMT study of Gerwer *et al.*[17] We find that vibrational averaging hardly affects the present cross sections, in contrast to what is seen in the MSM study. This exaggeration of the effects of vibrational averaging in the MSM treatment has also been noted in earlier studies on N_2.[21] Moreover, the shape resonance is much more pronounced and at higher energy than in the present study. Figure 6 also shows the experimental results of Samson *et al.*[5] and Brion *et al.*[6] The prominent structure in the experimental data indicates that autoionization may play a significant role in the low-energy cross section for the $X\,^2\Pi_g$ state of O_2^+. Holmes *et al.*[24] suggest that Rydberg states leading to the $b\,^4\Sigma_g^-$ ion (ionization potential equal to 18.17 eV) are responsible for some of the autoionization in the vibrationally unresolved angular distributions. Moreover, the high-resolution photoionization efficiency study of Dehmer *et al.*[25] identifies several other Rydberg states which may contribute to autoionization features in the vibrationally resolved photoionization cross sections. Clearly, the autoionization structure is rich and com-

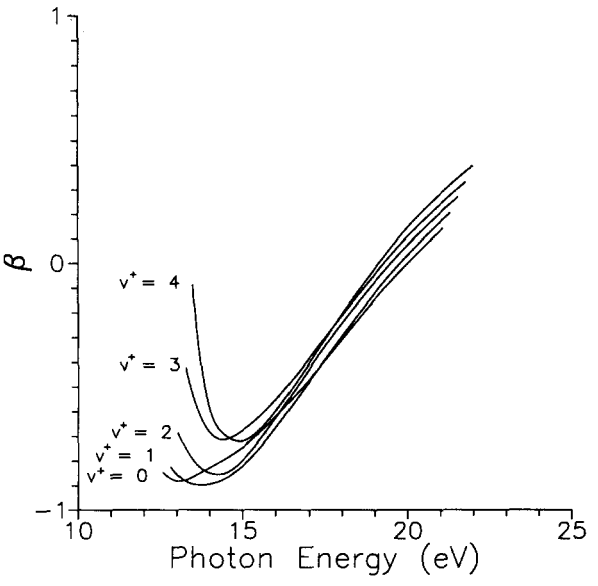

FIG. 8. Vibrationally resolved photoelectron asymmetry parameters (dipole length) leading to the $X\,^2\Pi_g$ state of O_2^+.

plex, and warrants further detailed experimental and theoretical study, as has been done on $3\sigma_g$ photoionization.[14]

In Fig. 7 we compare our calculated branching ratios to the line source data of Gardner *et al.*[26] As discussed above, autoionization structure complicates a comparison of the branching ratios with experimental data. Experiments employing a synchrotron source are needed to investigate the role of autoionization on these spectra.

Finally, in Fig. 8 we show our calculated vibrationally resolved photoelectron asymmetry parameters. These β's are strongly state dependent, particularly near threshold. This non-Franck–Condon behavior should be observable experimentally, barring additional complicating structure due to autoionization.

IV. CONCLUDING REMARKS

We have studied the vibrationally resolved cross sections and photoelectron angular distributions for photoionization leading to the $X\,^2\Pi_g$ ($v^+ = 0$–4) states of O_2^+. These studies were motivated by recent work showing the prominent role of a shape resonance in producing non-Franck–Condon effects in resonant multiphoton ionization of O_2 via the $C\,^3\Pi_g$ Rydberg state.[1–4] A σ_u shape resonance strongly influences these cross sections near the ionization threshold. This σ_u shape resonance leads to significant non-Franck–Condon behavior in ionization of the $1\pi_g$ level, and is evident in both the branching ratios and a vibrational state dependence of the photoelectron angular distributions below 21 eV photon energy. Comparison of our vibrationally resolved cross sections with available line-source data is seriously hindered by autoionization. Continuum source experiments are needed to further understand this structure, and to elucidate the shape-resonant continuum.

ACKNOWLEDGMENTS

This material is based upon research supported by the National Science Foundation under Grant No. CHE85-21391. The authors acknowledge use of the resources of the San Diego SuperComputer Center which is supported by the National Science Foundation. The authors also thank Dr. J. A. Stephens for helpful discussions and suggestions.

[1] P. J. Miller, L. Li, W. A. Chupka, and S. D. Colson, J. Chem. Phys. **89**, 3921 (1988).
[2] J. A. Stephens, M. Braunstein, and V. McKoy, J. Chem. Phys. **89**, 3923 (1988).
[3] P. J. Miller, W. A. Chupka, J. Winniczek, and M. G. White, J. Chem. Phys. **89**, 4058 (1988).
[4] M. Braunstein, J. A. Stephens, and V. McKoy, J. Chem. Phys. **90**, 633 (1989).
[5] J. A. R. Samson, J. L. Gardner, and G. N. Haddad, J. Electron Spectrosc. Relat. Phenom. **12**, 281 (1977).
[6] C. E. Brion, K. H. Tan, M. J. van der Wiel, and Ph. E. van der Leeuw, J. Electron Spectrosc. Relat. Phenom. **17**, 101 (1979).
[7] R. R. Lucchese, K. Takatsuka, and V. McKoy, Phys. Rep. **131**, 147 (1986).
[8] R. R. Lucchese, R. Raseev, and V. McKoy, Phys. Rev. A **25**, 2572 (1982).
[9] M. Braunstein, M. E. Smith, and V. McKoy, J. Chem. Phys. (to be published).
[10] T. H. Dunning, Jr., J. Chem. Phys. **53**, 2823 (1970).
[11] S. Huzinaga, *Gaussian Basis Sets for Molecular Calculations* (Elsevier, New York, 1984), p. 23.
[12] P. H. Krupenie, J. Phys. Chem. Ref. Data **1**, 423 (1972).
[13] T. Gustafsson, Chem. Phys. Lett. **75**, 505 (1980).
[14] P. Morin, I. Nenner, M. Y. Adam, M. J. Hubin-Franskin, J. Delwiche, J. Lefebvre-Brion, and A. Giusti-Suzor, Chem. Phys. Lett. **92**, 609 (1982).
[15] P. M. Dittman, D. Dill, and J. L. Dehmer, J. Chem. Phys. **76**, 5703 (1982).
[16] G. Raseev, H. Lefebvre-Brion, H. Le Rouzo, and A. L. Roche, J. Chem. Phys. **74**, 6686 (1981).
[17] A. Gerwer, C. Asaro, B. V. McKoy, and P. W. Langhoff, J. Chem. Phys. **72**, 713(1980).
[18] P. W. Langhoff, A. Gerwer, C. Asaro, and B. V. McKoy, Int. J. Quantum Chem. **13**, 645 (1979).
[19] U. Fano and J. W. Cooper, Rev. Mod. Phys. **40**, 441 (1968).
[20] J. L. Dehmer, D. Dill, and S. Wallace, Phys. Rev. Lett. **42**, 1005 (1979).
[21] R. R. Lucchese and V. McKoy, J. Phys. B **14**, L629 (1981).
[22] M. E. Smith, D. L. Lynch, and V. McKoy, J. Chem. Phys. **85**, 6455 (1986).
[23] See, for example, J. L. Dehmer, A. C. Parr, and S. H. Southworth, in *Handbook on Synchrotron Radiation*, edited by G. V. Marr (North-Holland, Amsterdam, 1986), Vol. II.
[24] R. M. Holmes and G. V. Marr, J. Phys. B **13**, 945 (1980).
[25] P. M. Dehmer and W. A. Chupka, J. Chem. Phys. **62**, 4525 (1975).
[26] J. L. Gardner and J. A. R. Samson, J. Electron Spectrosc. Relat. Phenom. **13**, 7 (1978).